Vibrational spectra of silicon cage clusters doped with Ti, Zr, or Hf

C. L. Reis[1] and J. M. Pacheco[1,2]
[1]*ATP Group and CMAF Complexo Interdisciplinar, Universidade de Lisboa, Av. Prof. Gama Pinto 2, P-1649-003 Lisboa, Portugal*
[2]*Departamento de Matemática e Aplicações, Universidade do Minho, 4710-057 Braga, Portugal*
(Received 25 June 2010; revised manuscript received 20 September 2010; published 20 October 2010)

We investigate the vibrational modes and infrared spectra of the exceptionally stable isovalent $X@Si_{16}$ (X=Ti, Zr, and Hf) nanoparticles, making use of first-principles density-functional theory. Our results predict the existence of high-intensity modes of low frequency. An estimate of the electron-phonon coupling strength λ is also provided based on a single-molecule method introduced recently. The large value of λ combined with predicted stability of bulk materials assembled with these nanoparticles suggest that these materials, when appropriately doped, may exhibit high-temperature superconducting properties.

DOI: 10.1103/PhysRevB.82.155440 PACS number(s): 61.46.−w, 36.40.−c, 71.20.Tx, 81.05.ub

I. INTRODUCTION

The $X@Si_{16}$ (X=Ti, Zr, and Hf) nanoparticles are the most stable neutral silicon clusters known to date. These metal-silicon clusters were predicted theoretically in 2001 (Ref. 1) and their stability has been confirmed experimentally using laser ablation[2] or magnetron cosputtering[3] techniques. Recently we investigated the possibility of using these nanotemplates to synthesize stable molecular solids.[4,5] Our results predict the formation of stable, wide band-gap materials crystallizing in hcp structures in which the nanoparticles bind weakly while maintaining their structural integrity. We also identified the "double-magic" nature of the isolated nanoparticles, which translate into low-chemical reactivity, large highest occupied molecular orbital-lowest unoccupied molecular orbital gaps and a self- organization of one-electron energy shells similar to a sphericallike jellium super atom, thus providing crucial hints toward the design of feasible new cluster assembled materials. In this work we use first-principles computer simulations within density functional theory to investigate the vibrational modes and infrared spectra of the isolated $X@Si_{16}$ (X=Ti, Zr, and Hf) clusters. These results further extend our previous theoretical characterization,[5] which can be used in conjunction with experiments to help identify these nanoparticles in the laboratory.[6,7]

Furthermore, making use of the vibrational spectra of these 17-atom clusters, we provide an estimate of the electron-phonon interaction strength λ of hypothetical superconductors assembled using these nanoparticles. Indeed, the recent discovery of superconductivity in boron-doped diamond[8,9] has once again revived the interest in covalent superconductors. Despite the low-superconducting transition temperature $T_c \approx 4$ K this result helped consolidating an increasingly unified approach to the understanding of superconductivity in covalent materials.[10,11] Covalent materials in appropriate conditions, such as intercalated graphite,[12,13] high-pressure silicon[14] and germanium, carbon nanotubes,[15] alkali-doped fullerides,[16,17] and magnesium diboride[18] are all superconductors. These materials have a lower T_c than the cuprates[19] but contrary to the cuprates case, the theoretical understanding of the superconducting mechanism in these materials seems solid. The Migdal-Eliashberg[20–22] theory of phonon mediated superconductivity coupled to modern electronic-structure density-functional theory (DFT) has been successfully applied to such covalent superconductors. As a consequence the field is now at a point where theorists can benefit from valuable insights of experiments and experiments can be designed to target materials with predesigned properties defined theoretically. Furthermore, molecular fragments can be used to estimate the electron-phonon coupling strength and even estimate T_c in hypothetical superconductors,[23,24] as we shall do in this work.

The paper is organized as follows: in Sec. II details of the method and simulations carried out are provided. Results and discussion are left to Sec. III whereas main conclusions and future prospects are postponed to Sec. IV.

II. METHODS

All *ab initio* calculations were performed within the generalized gradient approximation[25] to DFT using norm-conserving pseudopotentials[26] and a plane-wave basis.[27,28] An energy cut-off of 30.0 Hartree (816 eV) was used throughout, leading to well converged forces within 0.02 eV/Bohr.

A. Vibrational modes

The vibrational modes of frequency ω are obtained via a periodic displacement in time of each nuclei I

$$\mathbf{u}_I(t) = \mathbf{u}_I e^{i\omega t}.$$

This leads to the following eigenvalue equation:

$$-\omega^2 M_I \mathbf{u}_I = \sum_J \frac{\partial^2 E(\mathbf{R})}{\partial \mathbf{R}_I \partial \mathbf{R}_J} \mathbf{u}_J$$

which involves second derivatives of the ground-state energy $E(\mathbf{R})$ with respect to all N nuclei positions $\mathbf{R}_I$ ($I=1,\ldots,N$). Solving these equations leads to a set of frequencies $\omega^\nu(\nu=0,\ldots,3N)$ and corresponding normal modes $\mathbf{u}^\nu=\mathbf{u}^\nu_{\tau,\alpha}\mathbf{e}_\alpha$ involving the collective displacements of the nuclei ($\tau=0,\ldots,N$) along the Cartesian directions ($\alpha=x,y,z$).

B. Infrared spectrum

The absolute infrared intensity of the mode ν is given by[29]

$$I_\nu^{IR} = K \left| \sum_{\tau,\alpha,\beta} Z^*_{\tau,\alpha,\beta} u^\nu_{\tau,\beta} \right|^2$$

with $\tau=1,\ldots,N$ and $\alpha,\beta=x,y,z$. For intensities in $(D/\text{Å})^2\text{amu}^{-1}$ and Z in atomic units, $K=4.2056\times10^4$. The Born effective charge tensor $\mathbf{Z}^*$ is the second-order derivative of the energy with respect to both the electric field $\mathbf{G}$ and the nuclei displacement $\mathbf{R}_\tau$

$$Z^*_{\tau,\alpha,\beta} = \frac{\partial^2 E}{\partial G_\alpha \partial R_{\tau,\beta}}.$$

The second derivatives of the ground-state energy, with respect to atomic displacements and/or homogeneous electric fields are computed using density-functional perturbation theory (DFPT).[30,31]

C. Estimates of the electron-phonon coupling strength

Phonon mediated superconductivity is currently best described by the Eliashberg equations[20–22] which themselves are extensions of the BCS theory.[32] The key quantity in this theory is the electron-phonon spectral function α^2F. Assuming an isotropic gap function this quantity is given by

$$\alpha^2F(\omega) = \frac{1}{N_\uparrow(\varepsilon_F)} \sum_{\nu,n\mathbf{k},n'\mathbf{k}'} |g^\nu_{n\mathbf{k},n'\mathbf{k}'}|^2 \times \delta(\varepsilon_F - \varepsilon_{n\mathbf{k}})\delta(\varepsilon_F - \varepsilon_{n'\mathbf{k}'})\delta(\omega - \omega^\nu_{\mathbf{k}-\mathbf{k}'}), \quad (1)$$

where $N_\uparrow(\varepsilon_F)$ is the density of states (DOS) per spin at the Fermi level ε_F. The sum is done over all the phonon modes ν, electron bands n,n' and wave vectors $\mathbf{k},\mathbf{k}'$. The matrix elements $g^\nu_{n\mathbf{k},n'\mathbf{k}'}$ encode the scattering of an electron from a state $n\mathbf{k}$ to the state $n'\mathbf{k}'$ while emitting or absorbing a phonon of frequency ω, mode ν and wave vector $\mathbf{k}-\mathbf{k}'$ while the first two delta functions restrict the scattering to electrons in the Fermi surface. The double sum over the Brillouin zone in Eq. (1) requires a large number of matrix elements. Therefore in general an accurate calculation of α^2F is computationally very demanding. There are, however, some approximations that can be made which do not sacrifice most of the physics. The electron-phonon interaction is generally short ranged. In molecular solids, in particular, the dispersion of both the phonons and the electrons may be small. It is hence reasonable to consider only the coupling of the electrons to the intramolecular modes. This approach has been previously applied in several molecular systems using different metrics for the electron-phonon interaction strength.[17,23,24] Considering only intramolecular, i.e., Γ-point phonons ($\mathbf{q}=\mathbf{k}-\mathbf{k}'=0$, that is, a single k point, $\mathbf{k}=0$) but retaining the off-diagonal elements this function reduces to

$$\alpha^2F_\Gamma(\omega) = \frac{1}{N_\uparrow(\varepsilon_F)} \sum_{\nu,n,n'} |g^\nu_{n,n'}|^2 \times \delta(\varepsilon_F - \varepsilon_n)\delta(\varepsilon_F - \varepsilon_{n'})\delta(\omega - \omega^\nu). \quad (2)$$

The electron-phonon matrix elements are obtained from the self-consistent variation in the electronic potential by displacing a nucleus τ in the direction α. These, however, can be obtained directly from the DFPT computation of the vibrational modes. By transforming them to phonon coordinates and summing all the contributions from all atoms and directions the matrix elements for each mode ν are given by

$$g^\nu_{n,n'} = \sum_{\tau,\alpha} \frac{u^\nu_{\tau,\alpha}}{\sqrt{2M_\tau\omega^\nu}} \langle n| \frac{dV_{SCF}}{dR_{\tau,\alpha}} |n'\rangle.$$

In the calculation of $\alpha^2F(\omega)$ using Eq. (2) the delta functions have been replaced by normalized Gaussians with a smearing value of 0.01 Hartree. Using this value, the difference between the computed DOS of the isolated nanoparticles at the Fermi level and the corresponding DOS of the cluster assembled materials is minimized. From the Eliashberg spectral function the isotropic electron-phonon coupling strength can then be calculated

$$\lambda = 2\int_0^\infty d\omega \frac{\alpha^2F(\omega)}{\omega}.$$

Molecular materials assembled with the $X@Si_{16}$ (X=Ti, Zr, and Hf) nanoparticles are predicted to be insulators.[4,5] However, by appropriately doping these materials with electron donor atoms one hopefully expects these extra electrons from the dopant atoms to occupy some conduction bands of the bulk materials without altering much the overall band structure. Both $\alpha^2F_\Gamma(\omega)$ and λ have an implicit dependence on the Fermi level: $\alpha^2F_\Gamma(\omega)=\alpha^2F_\Gamma(\omega;\varepsilon_F)$ and $\lambda=\lambda(\varepsilon_F)$. By varying ε_F then $\lambda(\varepsilon_F)$ can be estimated for a set of electronic levels in the hypothetical conducting material. In particular this information can be used to maximize the electron-phonon coupling strength. Choosing carefully the number of valence electrons of the dopant atoms we can try to maximize the electron-phonon coupling strength and therefore the superconducting transition temperature since in the strong coupling regime $T_c \sim \sqrt{\lambda\langle\omega^2\rangle}$. This methodology has been recently employed by Moussa and Cohen[24] to estimate the electron-phonon coupling and possible superconductivity in hypothetical covalent materials. These authors used a somewhat different metric for the electron-phonon coupling strength (which is independent of the phonon details), and also an upper bound of T_c: see Eqs. (2) and (1), respectively, of Ref. 24. A similar methodology was also used to successfully describe superconductivity in boron-doped diamond[33] in this case with a Γ-point approximation to the Eliashberg spectral function. In line of what was done in Ref. 33 we choose to retain the phonon details of the molecule on the calculation of λ but use a single k point.

D. Estimates of the superconducting transition temperature

The superconducting transition temperature T_c was estimated by solving numerically[34,35] the Eliashberg gap equation for an electron-phonon spectral function $\alpha^2F(\omega)$ and a parameter μ^* which is the coulomb pseudopotential opposing superconductivity. μ^* is typically between 0.1 and 0.15 in metals and variations in this interval only affect the determination of T_c in a few percent. We use $\mu^*=0.1$ in the estimation of T_c. The isotropic linearized Eliashberg gap equation in the Mastsubara representation can be written as

$$\rho\bar{\Delta}(i\omega_n) = \sum_{m=-N-1}^{N} \left[\lambda(n-m) - \mu^*(N) - \frac{\delta_{mn}|\tilde{\omega}_n|}{\pi T} \right] \times \bar{\Delta}(i\omega_m), \tag{3}$$

where $\bar{\Delta}$ is a modified gap parameter

$$\bar{\Delta}(i\omega_n) = \frac{|\tilde{\omega}_n/\omega_n|\Delta(i\omega_n)}{|\tilde{\omega}_n| + \pi T\rho}$$

ρ is a pair-breaking parameter and $\tilde{\omega}_n$ is a renormalized frequency

$$\tilde{\omega}_n = \omega_n Z(i\omega_n) = \omega_n + \pi T\left[\lambda(0) + 2\sum_{l=1}^{n} \lambda(l) \right],$$

where $\omega_n = 2\pi nT$. The parameter $\mu^*(N)$ is the rescaled μ^* taking into account the necessary numerical truncation at ω_N

$$\frac{1}{\mu^*(N)} = \frac{1}{\mu^*} + \ln\left(\frac{\sqrt{\langle w\rangle^2}}{\omega_N} \right)$$

with the moments of the spectral function given by

$$\langle \omega^n \rangle = \frac{2}{\lambda}\int_0^\infty d\omega \alpha^2 F(\omega)\omega^{n-1}.$$

Finally the electron-phonon interaction parameters $\lambda(n)$ are defined by:

$$\lambda(n) = 2\int_0^\infty d\omega \frac{\alpha^2 F(\omega)\omega}{\omega^2 + (2\pi nT)^2}.$$

After a simple manipulation Eq. (3) can be cast as a simple eigenvalue problem

$$\sum_{n=0}^{N} (K_{mn} - \rho\delta_{mn})\bar{\Delta}(i\omega_n) = 0 \tag{4}$$

with

$$K_{mn} = \lambda(m-n) + \lambda(m+n+1) - 2\mu^*(N) - \delta_{mn}\left[2m + 1 + \lambda(0) + 2\sum_{l=1}^{m} \lambda(l) \right].$$

The pair-breaking parameter ρ is only a simple mathematical device introduced to solve the Eliashberg equation. At the critical temperature it becomes zero. T_c is then determined by lowering T from a sufficiently large value. At this initial temperature all the eigenvalues of Eq. (4) are negative. However, as T is lowered toward T_c one of the eigenvalue becomes zero while all the others remain negative.

III. RESULTS AND DISCUSSION

The structures of the $X@Si_{16}$ (X=Ti, Zr, and Hf) nanoparticles were obtained using the procedure outlined in a previous work.[5] Following the ground-state structure determination, a computation of the second-order derivatives of the energy with respect to this set of coordinates was carried out. The mixed second-order derivatives of the energy with respect to the coordinates and the electric field were also determined. The set of frequencies ω^ν, normal mode displacements $\mathbf{u}^\nu$ and the Born effective charges $\mathbf{Z}^*$ were then determined from the second order derivatives of the ground-state energy of each nanoparticle.

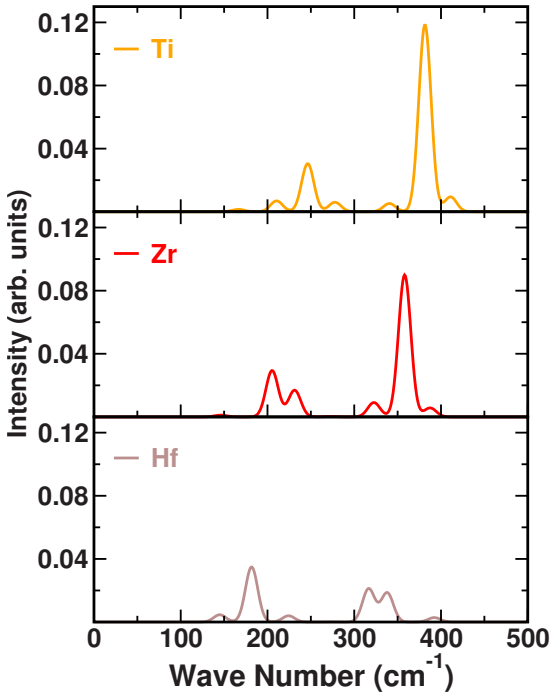

FIG. 1. (Color online) The calculated infrared spectrum of the $X@Si_{16}$ (X=Ti, Zr, and Hf) nanoparticles.

In Fig. 1 we show the results of the calculation of the infrared spectrum using the procedure described in the previous section. To facilitate the comparison with experiments and previous theoretical work, the calculated intensities are replaced with normalized Gaussian functions with intrinsic width 10 cm^{-1}. In all three cases the normal modes have frequencies which are low compared to, e.g., isolated fullerenes, exhibiting sizable intensity ~200 cm^{-1}. This picture is consistent with a weaker bonding of the silicon atoms in the $X@Si_{16}$ (X=Ti, Zr, and Hf) nanoparticles compared to the carbon atoms in the fullerene clusters. The IR spectrum for $Ti@Si_{16}$ depicted in the upper panel of Fig. 1 is nearly identical to the one obtained by Nakajima and co-workers[36] using a localized basis set method. One interesting feature apparent in Fig. 1 is a progressive softening of the frequency spectrum with the increasing mass of the central metal atom. This is accompanied with a simultaneous decrease in IR activity which is most pronounced for $Hf@Si_{16}$. The peaks of highest intensity at 380 cm^{-1} and 360 cm^{-1}, for $Ti@Si_{16}$ and $Zr@Si_{16}$, respectively, correspond to the three normal modes depicted in the upper part of each panel of Fig. 2. In the case of $Ti@Si_{16}$ these are essentially displacements of the central metal atom in the cluster with minor rearrangements of the surrounding silicon atoms. For the $Zr@Si_{16}$ the movement of the central metal atom is accompanied by a more sizable distortion of the silicon cage. This is also the case for the three modes corresponding to the second most intense peak for both $Ti@Si_{16}$ and $Zr@Si_{16}$ at 246 cm^{-1}

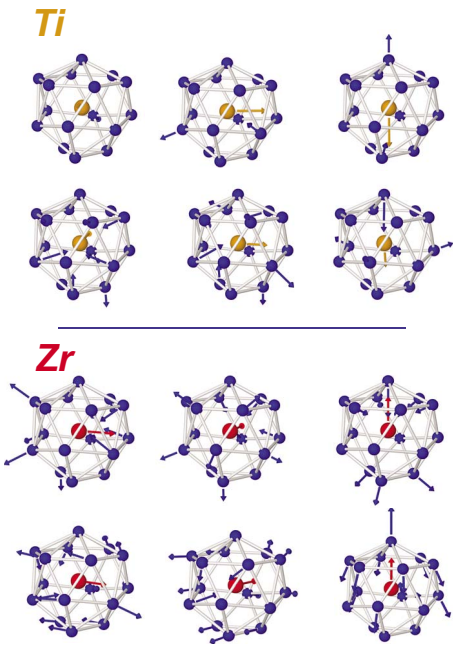

FIG. 2. (Color online) Selected normal modes for the $Ti@Si_{16}$ (upper panel) and $Zr@Si_{16}$ (lower panel) nanoparticles. In each panel the three top modes correspond to the peak of highest IR activity whereas the lower three modes correspond to second most intense peak.

and 205 cm^{-1}, respectively. In the case of $Hf@Si_{16}$ the peak of highest IR activity is located at 180 cm^{-1}. These modes are depicted in the upper part of Fig. 3 whereas the second most intense peaks correspond to the six normal modes depicted in the lower part of Fig. 3.

Using the procedure described in Sec. II we estimate the electron-phonon coupling strength λ as function of the electronic level for the isolated $X@Si_{16}$ (X=Ti, Zr, and Hf) nanoparticles. The results are given in Fig. 4. The vertical

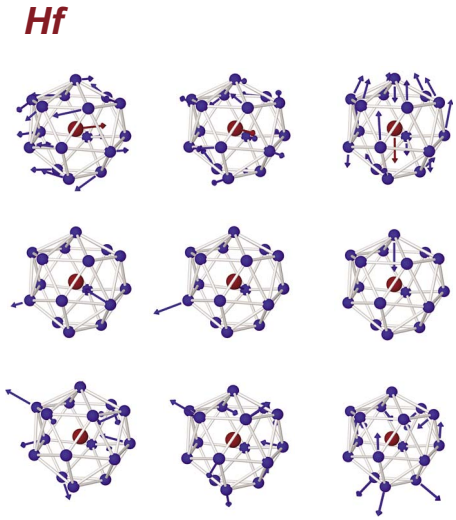

FIG. 3. (Color online) Selected normal modes for the $Hf@Si_{16}$ nanoparticles. The three top modes correspond to the peak of highest IR activity whereas the lower six modes correspond to second most intense peaks.

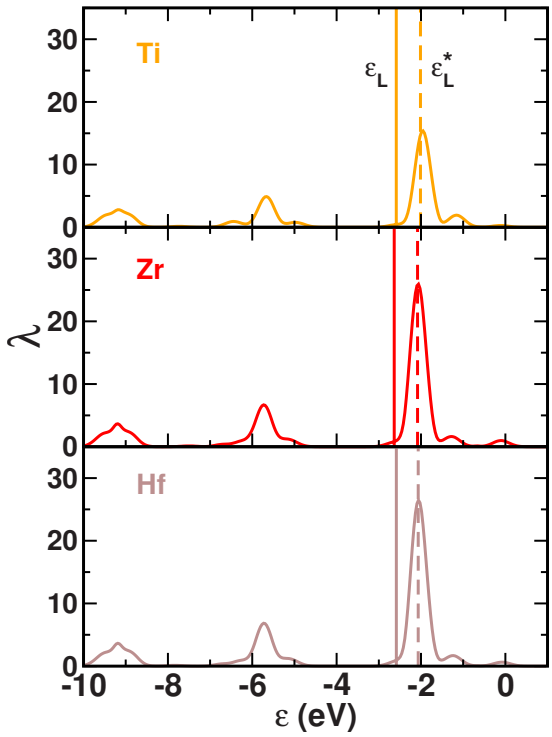

FIG. 4. (Color online) Calculated electron-phonon coupling as a function of the molecular orbital energy level ε for the isolated $X@Si_{16}$ (X=Ti, Zr, and Hf) nanoparticles. The solid (dashed) lines represent the energy $\varepsilon_L(\varepsilon_L^*)$ of the first (second) set of degenerate unoccupied molecular orbitals.

bars are placed at the energy ε_L of the first set of threefold degenerate unoccupied molecular orbitals. The calculated electron-phonon coupling strength for this level, $\lambda(\varepsilon_L)$ corresponds to the weak coupling regime $[\lambda(\varepsilon_L)<1]$ in all three cases. Very large values for λ occur, however, for the second set of threefold degenerate unoccupied molecular orbitals ε_L^*. These correspond to the large peaks in Fig. 4. This result is rather unexpected given that these large values for the electron-phonon coupling strength are unusual for covalent materials. We note, however, that by optimizing electron or hole doping using a similar procedure, Moussa and Cohen obtained recently[24] unusually large values for λ for hypothetical materials based on C_4O_6 molecular units. A value as large as $\lambda \approx 70$ was reported together with a room temperature T_c. The calculated Eliashberg spectral functions for the second set of threefold degenerate unoccupied molecular orbitals $\alpha^2F_\Gamma(\omega;\varepsilon_F^*)$ are depicted in Fig. 5. The large peaks at 33 cm^{-1} for $Ti@Si_{16}$ and 26 cm^{-1} for $Zr@Si_{16}$ and $Hf@Si_{16}$, respectively, are responsible for a large part of the calculated electron-phonon coupling strength (≈90%).

These results strongly suggest that attempts to synthesize molecular materials assembled with the $X@Si_{16}$ (X=Ti, Zr, and Hf) nanoparticles should be carried out. In a previous work[4,5] we predicted that these materials should be stable under normal pressure and room temperature. The calculated band gaps 1.3 eV ($Ti@Si_{16}$) and 1.6 eV ($Zr@Si_{16}$ and $Hf@Si_{16}$) indicate that these materials should be insulators. The predicted bulk structure is hexagonal close packed with a distance between nanoparticles in the bulk ≈17 Bohr. This

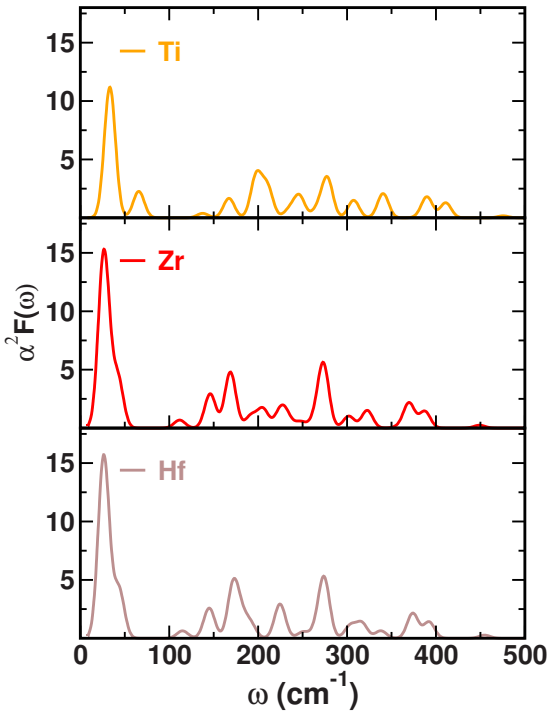

FIG. 5. (Color online) Eliashberg spectral functions $\alpha^2F_\Gamma(\omega;\varepsilon_F^*)$ at maximal electron-phonon coupling strength for the isolated $X@Si_{16}$ (X=Ti, Zr, and Hf) nanoparticles.

large space between nanoparticles in the bulk opens an interesting possibility. Electron donor atoms can be placed interstitially in the molecular materials (see Fig. 6). Assuming no significant structural transformation, the extra electrons from the dopant atoms will hopefully populate some of the conduction bands of the previously insulating molecular materials. Furthermore the number of valence electrons of the dopant atoms can be adjusted to obtain a maximal electron-

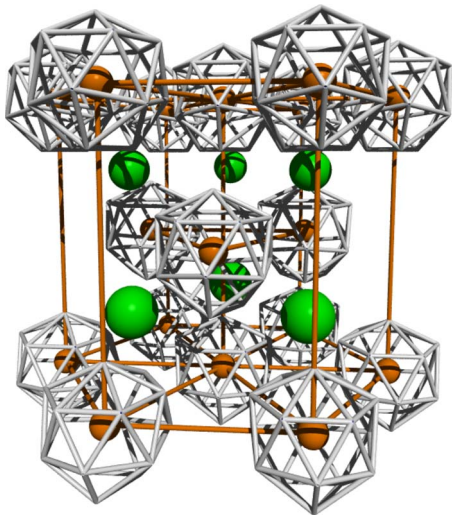

FIG. 6. (Color online) Electron donor atoms (larger spheres) can be inserted in the spaces between $X@Si_{16}$ (X=Ti, Zr, and Hf) nanoparticles in the bulk. The nanoparticles are predicted to assemble in stable hexagonal closed packed structures. The representation is in the conventional hexagonal cell.

TABLE I. Estimated electron-phonon coupling strength λ and superconducting temperature T_c for hypothetical materials assembled with $X@Si_{16}$ (X=Ti, Zr, and Hf) clusters and doped with electron donor atoms. The results are calculated at maximal electron-phonon coupling strength from $\alpha^2F_\Gamma(\omega;\varepsilon_F^*)$.

$X@Si_{16}$	λ	T_c (K)
Ti	14.8	87
Zr	25.9	87
Hf	26.5	80

phonon coupling. If we further assume that the calculated $\alpha^2F_\Gamma(\omega;\varepsilon_F^*)$ is a reasonable approximation to the spectral functions of hypothetical materials assembled with the $X@Si_{16}$ (X=Ti, Zr, and Hf) nanoparticles and doped with electron donor for maximal coupling then the superconducting transition temperature can also be estimated by solving numerically the Eliashberg equations for the model spectral function $\alpha^2F_\Gamma(\omega;\varepsilon_F^*)$. These estimates are summarized in Table I. The obtained T_c values are unusually high for covalent materials. We emphasize that these are only estimates of possible high-temperature superconductivity in molecular materials assembled with the $X@Si_{16}$ (X=Ti, Zr, and Hf) nanoparticles. It is also important to note that the class of molecular, narrow bandwidth superconductors is experimentally observed to be close to a metal-insulator transition.[37] If the bandwidth is too narrow, superconductivity may not occur without applied pressure. Additionally, important properties such as the structure of the doped molecular material and its structural stability, electronic band structure and a computation of the Eliashberg spectral function using Eq. (1) for the bulk material should be carried out for a more accurate determination of the superconducting transition temperature. We believe that the results obtained here justify the significant increase in computational effort to pursue such a program. Work along these lines is in progress.

IV. CONCLUSIONS

Making use of first-principles computer simulations in the framework of density-functional theory we calculated the vibrational modes and infrared spectra of the exceptionally stable isovalent $X@Si_{16}$ (X=Ti, Zr, and Hf) nanoparticles. Our results predict modes with sizable intensity and low frequency $\omega<500$ cm^{-1}. Based on these results, we used the framework developed in Refs. 24 and 33 to carry out estimates of the electron-phonon coupling strengths for the intramolecular modes. Given the large values obtained for λ we explored the possibility that appropriately doped bulk materials assembled with the $X@Si_{16}$ (X=Ti, Zr, and Hf) nanoparticles can exhibit high-temperature superconducting properties. Estimates of the critical superconducting transition temperature were obtained by solving numerically the Eliashberg equations for an approximated spectral function. The preliminary values for λ and T_c can be unusually high for covalent materials. These are very encouraging results

and we further hope that they stimulate experimental work aimed at synthesizing these materials in the laboratory, as well as the pursuit of computer simulations to obtain more accurate values for these quantities.

ACKNOWLEDGMENT

Financial support from FCT-Portugal is gratefully acknowledged.

[1] V. Kumar and Y. Kawazoe, Phys. Rev. Lett. **87**, 045503 (2001).
[2] K. Koyasu, J. Atobe, M. Akutsu, M. Mitsui, and A. Nakajima, J. Phys. Chem. A **111**, 42 (2007).
[3] J. Lau, K. Hirsch, Ph. Klar, A. Langenberg, F. Lofink, R. Richter, J. Rittmann, M. Vogel, V. Zamudio-Bayer, and T. Möller, Phys. Rev. A **79**, 053201 (2009).
[4] C. L. Reis, J. L. Martins, and J. M. Pacheco, Phys. Rev. B **76**, 233406 (2007).
[5] C. L. Reis and J. M. Pacheco, J. Phys.: Condens. Matter **22**, 035501 (2010).
[6] G. K. Gueorguiev and J. M. Pacheco, J. Chem. Phys. **114**, 6068 (2001).
[7] G. K. Gueorguiev and J. M. Pacheco, Phys. Rev. B **68**, 241401 (2003).
[8] E. A. Ekimov, V. A. Sidorov, E. D. Bauer, N. N. Melnik, N. J. Curro, J. D. Thompson, and S. M. Stishov, Nature (London) **428**, 542 (2004).
[9] Y. Takano, T. Takenouchi, S. Ishii, S. Ueda, T. Okutsu, I. Sakaguchi, H. Umezawa, H. Kawarada, and M. Tachiki, Diamond Relat. Mater. **16**, 911 (2007).
[10] W. E. Pickett, Physica C **468**, 126 (2008).
[11] M. L. Cohen, J. Supercond. Novel Magn. **19**, 283 (2006).
[12] N. Emery, C. Hérold, J.-F. Marêché, and P. Lagrange, Sci. Technol. Adv. Mater. **9**, 044102 (2008).
[13] I. T. Belash, O. V. Zharikov, and A. V. Palnichenko, Synth. Met. **34**, 455 (1990).
[14] K. J. Chang, M. M. Dacorogna, M. L. Cohen, J. M. Mignot, G. Chouteau, and G. Martinez, Phys. Rev. Lett. **54**, 2375 (1985).
[15] Z. K. Tang, L. Zhang, N. Wang, X. X. Zhang, G. H. Wen, G. D. Li, J. N. Wang, C. T. Chan, and P. Sheng, Science **292**, 2462 (2001).
[16] T. Palstra, O. Zhou, Y. Iwasa, P. E. Sulewski, R. M. Fleming, and B. R. Zegarski, Solid State Commun. **93**, 327 (1995)
[17] O. Gunnarsson, Rev. Mod. Phys. **69**, 575 (1997).
[18] J. Nagamatsu, N. Nakagawa, T. Muranaka, and J. Akimitsu, Nature (London) **410**, 63 (2001).
[19] J. G. Bednorz and K. A. Müller, Z. Phys. B: Condens. Matter **64**, 189 (1986).
[20] G. M. Eliashberg, Sov. Phys. JETP **11**, 696 (1960).
[21] G. M. Eliashberg, Zh. Eksp. Teor. Fiz. **38**, 966 (1960).
[22] D. J. Scalapino, J. R. Schrieffer, and J. W. Wilkins, Phys. Rev. **148**, 263 (1966).
[23] N. A. Romero, J. Kim, and R. M. Martin, Phys. Rev. B **70**, 140504(R) (2004).
[24] J. E. Moussa and M. L. Cohen, Phys. Rev. B **78**, 064502 (2008).
[25] J. P. Perdew, K. Burke, and M. Ernzerhof, Phys. Rev. Lett. **77**, 3865 (1996).
[26] N. Troullier and J. L. Martins, Phys. Rev. B **43**, 1993 (1991).
[27] X. Gonze, J.-M. Beuken, R. Caracas, F. Detraux, M. Fuchs, G.-M. Rignanese, L. Sindic, M. Verstraete, G. Zerah, F. Jollet, M. Torrent, A. Roy, Ph. Ghosez, J.-Y. Raty, and D. C. Allan, Comput. Mater. Sci. **25**, 478 (2002).
[28] X. Gonze, G.-M. Rignanese, M. Verstraete, J.-M. Beuken, Y. Pouillon, R. Caracas, F. Jollet, M. Torrent, G. Zerah, M. Mikami, Ph. Ghosez, M. Veithen, J.-Y. Raty, V. Olevano, F. Bruneval, L. Reining, R. Godby, G. Onida, D. R. Hamann, and D. C. Allan, Z. Kristallogr. **220**, 558 (2005).
[29] D. Porezag and M. R. Pederson, Phys. Rev. B **54**, 7830 (1996).
[30] X. Gonze, Phys. Rev. B **55**, 10337 (1997).
[31] X. Gonze and C. Lee, Phys. Rev. B **55**, 10355 (1997).
[32] J. Bardeen, L. N. Cooper, and J. R. Schrieffer, Phys. Rev. **108**, 1175 (1957).
[33] J. E. Moussa and M. L. Cohen, Phys. Rev. B **77**, 064518 (2008).
[34] P. B. Allen and R. C. Dynes, Phys. Rev. B **12**, 905 (1975).
[35] S. G. Louie and M. L. Cohen, Solid State Commun. **22**, 1 (1977).
[36] S. Furuse, K. Koyasu, J. Atobe, and A. Nakajima, J. Chem. Phys. **129**, 064311 (2008).
[37] Y. Takabayashi, A. Y. Ganin, P. Jeglič, D. Arčon, T. Takano, Y. Iwasa, Y. Ohishi, M. Takata, N. Takeshita, K. Prassides, and M. J. Rosseinsky, Science **323**, 1585 (2009).